P H Y S I C A L   R E V I E W   L E T T E R S

Hierarchical Organization Unveiled by Functional Connectivity in Complex Brain Networks

Changsong Zhou,[1] Lucia Zemanová,[1] Gorka Zamora,[1] Claus C. Hilgetag,[2] and Jürgen Kurths[1]

[1]*Institute of Physics, University of Potsdam PF 601553, 14415 Potsdam, Germany*
[2]*International University Bremen, Campus Ring 6, RII-116, D-28759 Bremen, Germany*

How do diverse dynamical patterns arise from the topology of complex networks? We study synchronization dynamics in the cortical brain network of the cat, which displays a hierarchically clustered organization, by modeling each node (cortical area) with a subnetwork of interacting excitable neurons. We find that in the biologically plausible regime the dynamics exhibits a hierarchical modular organization, in particular, revealing functional clusters coinciding with the anatomical communities at different scales. Our results provide insights into the relationship between network topology and functional organization of complex brain networks.

Studying the impact of complex network topology on dynamical processes is of fundamental importance for understanding the functions of real-world systems [1]. Synchronization of complex networks has been intensively investigated as a universal concept in many disciplines [2], particularly in neuroscience [3]. Most previous studies used generic oscillators as the nodes of typical network models, such as small-world (SW) and scale-free networks, and analyzed the ability to achieve idealized complete synchronization or coherent collective oscillations. However, many realistic network systems display several levels of topological organization not well accounted for by typical network models [4]. The oscillatory dynamics cannot be sufficiently described by low-dimensional oscillators, and the synchronization behavior is often far from the ideal situations [3]. In spite of recent efforts to examine the regimes outside [5] or during the transient to global synchronization [6], the relationship between network topology and synchronization behavior remains an important open problem.

The cerebral cortex of mammalian brains is an excellent example of such realistic complex systems. Cortical connectivity is organized into a hierarchy, from the microscopic cellular level via the mesoscopic level of local neural circuits and columns to the macroscopic level of nerve fiber projections between brain areas [7]. While details at the first two levels are still largely missing, extensive information has been collected about the latter level in the brains of animals, such as the cat and the macaque monkey [8]. The experimentally observed brain activity is characterized by synchronization phenomena over a wide range of spatial and temporal scales [9]. The analysis of the anatomical connectivity of the mammalian cortex [8] and the functional connectivity of the human brain [10] have shown that both share typical features of many complex networks. However, the relationship between the anatomical and functional connectivities remains one of the major challenges in neuroscience [3].

Our attempt in this Letter is to focus on the highest structural level, i.e., the systems level of corticocortical connections. We employ the known cortical network of the cat and simulate the dynamics of each node (cortical area) by a subnetwork of interacting excitable neurons. The cortex of the cat can be parcelated into 53 areas which are linked by about 830 fiber connections of different densities [7]. It forms a weighted complex network [Fig. 1(a)] and displays typical SW properties [11,12]. The system also exhibits a hierarchically clustered organization [12,13]. There exist a small number of clusters that broadly agree with the four functional cortical subdivisions, i.e., visual cortex (V), auditory (A), somato-motor (SM), and fronto-limbic (FL). We refer to the topological clusters as *communities* [14], to distinguish them from the dynamical clusters. Among the four communities, A is much less connected, while V, SM, and FL are densely interconnected [Fig. 1(b)]. We will show that the dynamical behavior in this system reveals different scales in the network topology.

The subnetwork representing each cortical area is arranged as a SW topology [15], i.e., a regular array of
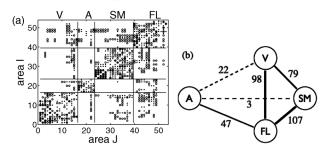

FIG. 1. (a) Anatomical connection matrix M^A of the cortical network of the cat brain. The symbols represent different densities (weights) of the fiber connections: 1 (•, sparse), 2 (∘, intermediate), and 3 (∗, dense). The organization of the system into four topological communities (functional subsystems V, A, SM, and FL) is indicated by the solid lines. (b) The number of connections between the four communities.
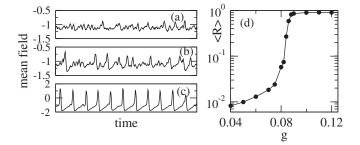
FIG. 2. Mean activity X of one area at various couplings:
(a) $g = 0.06$, (b) $g = 0.082$, and (c) $g = 0.09$. (d) The average
correlation coefficient $\langle R \rangle = \frac{1}{N(N-1)} \sum_{I \neq J}^{N} R(I, J)$ ($N = 53$) vs g.

FIG. 3. Correlation matrices $R(I, J)$ at (a) weak coupling $g = 0.06$ and (b) strong coupling $g = 0.09$.

$N_a (= 200)$ neurons with a mean degree $k_a (= 12)$ that is
rewired with a probability $p (= 0.3)$. Such a topology in-
corporates basic biological features (neurons are connected
mainly to their spatial neighbors but also form a few long-
range connections [16]) and is found to enhance synchro-
nization of neural networks [17]. Our model also includes
other realistic, experimentally observed features, e.g., 25%
of the N_a neurons are inhibitory, and only a small number
of neurons (about 5%) in one area receive excitatory
synapses from connected areas [18]. For simplicity of
modeling the dynamics at the systems level, we assume
that the output signal from one area is the mean activity of
the area, projecting to other areas with the connection
weights in Fig. 1(a). Individual neurons are described by
the FitzHugh-Nagumo (FHN) model [19] with nonidenti-
cal excitability. A weak Gaussian white noise is added to
each neuron to generate sparse, Poisson-like irregular
spiking patterns in isolated FHN neurons, as seen in real-
istic neurons. Thus, our model of a cat cortex is a *network
of networks* of noisy excitable neurons. The results at the
systems level, as reported below, do not depend critically
on the neuron model, the subnetwork parameters, and de-
tailed coupling (electrical vs chemical) between neurons.

The average coupling strength g between any pair of
neurons is the only control parameter in our simulations,
and it defines the mutual excitation among the neurons. At
small g (e.g., $g = 0.06$), a neuron is not often excited by
the noise-induced spiking of its connected neighbors, so
the synchronization within and between the subnetworks is
weak. This is shown by small fluctuations of the mean
activity X_I of each area (average potential, analogy of
electroencephalogram [20]) [Fig. 2(a)] and a small average
correlation coefficient $\langle R \rangle$ among X_I [Fig. 2(d)].
Synchronization in the subnetwork is manifested by
some apparent peaks in X [Fig. 2(a)]. Increasing g, the
synchronization becomes stronger with more frequent and
larger peaks in X_I [Fig. 2(b)], and, at large enough g, the
neurons are mutually excited, achieving both strongly
synchronized and regular spiking behavior [Fig. 2(c)].

The pattern of the correlation $R(I, J)$ between the mean
activities X_I and X_J shows clustered dynamics. Figure 3(a)
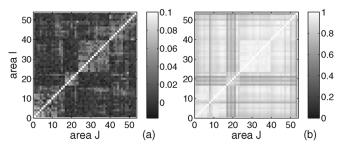suggests that the weak-coupling dynamics has a nontrivial

organization and a close relationship with the underlying
network topology. The distribution of R among all pairs of
areas displays a Gaussian peak around zero but with a long
tail towards large values [Fig. 4(a), solid line]. These
values are significant compared to R of surrogate data by
random shuffling of the time series X_I [Fig. 4(a), dashed-
dotted line]. The weak-coupling regime is biologically
more realistic with a low frequency and irregular spiking
behavior. Here the propagation of a signal between con-
nected areas is mediated by synchronized activities (peaks
in X), and a temporal correlation is most likely established
when the receivers produce similar synchronized activities
by this input or when two areas are excited by correlated
signals from common neighbors. Because of the weak
coupling and the existence of subnetworks, such a syn-
chronized response does not always occur, and a local
signal (excitation) does not propagate through the whole
network. With strong coupling, the signal can propagate
through the whole network, as corresponds to pathological
situations, such as epileptic seizures [21].

Based on the argument of signal propagation, we can
distinguish three cases for any pair of areas in the cat
network: reciprocal projections (P2), unidirectional cou-
plings (P1), and nonconnection (P0). The distributions of R
for these three cases display well-separated peaks in the
weak-coupling regime [Fig. 4(a)]. At strong coupling, the
separation is no longer pronounced. We extract a *func-
tional network* M^F [10] by applying a threshold R_{th} to
the correlation R; i.e., two areas are considered to be
functionally connected if $R(I, J) \geq R_{th}$ [$M^F(I, J) = 1$].
We compare the anatomical network M^A and the functional
networks M^F at various R_{th} and examine how the various
levels of synchronization reveal different scales in the
network topology.

Take $g = 0.07$ as a typical case. When R_{th} is close to the
maximal value of R, only some P2 areas are functionally
connected; e.g., at $R_{th} = 0.07$, about 2/3 of areas but only
10% of the P2 links are present in M^F [Fig. 4(c)].
Interestingly, within each anatomical community V, A,
SM, and FL, a core subnetwork is functionally manifested
in the form of connected components without intercom-
munity connections. At lower R_{th}, more areas from the
respective communities are included into these compo-
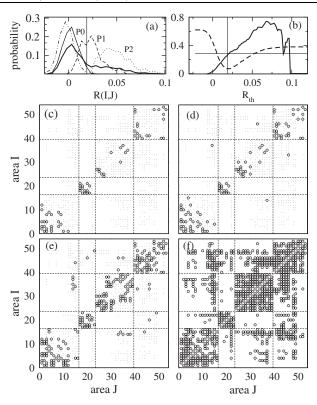nents, and a few intercommunity connections appear to

FIG. 4. (a) Distribution of the correlation R ($g = 0.07$) for all nodes (solid line), P2 (dotted line), P1 (dashed line), and P0 (light solid line) and for surrogate data (dashed-dotted line). (b) Modularity Q^F (solid line) and Hamming distance H (dashed line) vs R_{th}. The horizontal solid line is Q^{all}. The vertical solid lines in (a) and (d) denote the natural threshold $R_{th} = 0.019$. The functional networks M^F ($\circ$) at various thresholds (c) $R_{th} = 0.070$, (d) $R_{th} = 0.065$, (e) $R_{th} = 0.055$, and (f) $R_{th} = 0.019$. The small dots indicate the anatomical connections.

join them [Fig. 4(d)]. This observation suggests the existence of a core subnetwork within each community that performs specialized functions. At $R_{th} = 0.055$, only about 1/3 of the anatomical P2 links and very few P1 links can already connect all of the cortical areas into a single functional network. Moreover, the communication of the whole network is still mediated by only a few intercommunity connections; i.e., the functional network is highly clustered [Fig. 4(e)]. At a smaller $R_{th} = 0.019$, all P2 links are just fully expressed and also about 70% of P1 and 4% of P0 links. Thus, the functional connectivity agrees rather faithfully with the anatomical network [Fig. 4(f)]. The closeness between them is confirmed by a very small Hamming distance $H = 0.074$ [22], which is almost minimal with respect to R_{th} [Fig. 4(b)]. It is important to note that this value of R_{th} is exactly where the distribution of R for P2 separates from that of the surrogate data (at a significance level $\approx 0.4\%$) [Fig. 4(a)]. We find that such a natural choice of R_{th} always reproduces well the network topology with $H \approx 0.06$ for different coupling strengths $0.04 \leq g \leq 0.08$.

The formation of communities in complex networks can be quantified by modularity Q [14]:

$$Q = \sum_k e_{kk} - a_k^2, \tag{1}$$

where $a_k = \sum_l e_{kl}$ and e_{kl} is the fraction of all links in the network that connect the nodes between the communities k and l. To characterize the formation of functional clusters according to the anatomical communities [Figs. 4(c)–4(f)], we consider the four communities ($k = $ V, A, SM, FL) and measure the functional modularity Q^F based on the functional networks M^F. In a broad range of R_{th}, Q^F is much larger than Q^{all} computed using the full anatomical (binary) connectivity of M^A, and they coincide at the natural threshold $R_{th} = 0.019$ [Fig. 4(b)]. This provides meaningful insights into how densely connected cortical subsystems can perform highly specialized functions by a subset of areas and connections.

The above analysis suggests that the dynamics of the network is hierarchically clustered. A typical hierarchical tree in the weak-coupling regime is shown in Fig. 5(a). At each level of the tree, a set of N_c clusters is detected, and the question is what the underlying topological links within and across these dynamical clusters are. We calculate both the anatomical modularity Q^A [using matrix $M^A(I, J)$] and the functional modularity Q^C [using matrix $R(I, J)$]. We define Q^C by an extension of Q in Eq. (1) with

$$e_{kl} = \sum_{I \neq J} R(I, J): I \in k, \quad J \in l, \quad \text{and} \quad k, l = 1, \ldots, N_c. \tag{2}$$

So e_{kl} is the fraction of the total strength of correlation between the communities k and l. Strikingly, at different levels of the hierarchy (varying N_c), Q^C and Q^A follow each other closely [Fig. 5(b)]. This provides strong evidence that the dynamical organization reveals hierarchical scales in the network topology. At $N_c = 4$, Q^C and Q^A are maximal, approaching Q^{all} of the four communities in the anatomical network. Thus, the most prominent dynamical
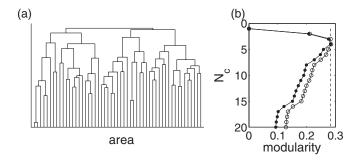

FIG. 5. (a) The hierarchical tree of the dynamical clusters at $g = 0.07$. (b) Modularities Q^C ($\circ$) and Q^A ($\bullet$) vs the number of clusters N_c. The dashed line denotes Q^{all}.

clusters are consistent with the four known anatomical communities.

The behavior described above is common for coupling strength $g \lesssim 0.08$, although the correlation R increases with g. However, for $g \gtrsim 0.084$, the system achieves strong local synchronization, and each area becomes significantly correlated with the rest of the network. The three communities V, SM, and FL join to form a hypercluster while A remains relatively independent, as reflected by the intercommunity connectivity in Fig. 1(b).

We stress that the striking relationship between the dynamical organization and network topology in the weak-coupling regime results from our biologically plausible modeling of the cortical areas as subnetworks of excitable neurons. It might be reasonable to model the mean activity of each area by a single oscillator, e.g., the periodic neural mass oscillators for modeling neural rhythms [23]. Using such a model and generic oscillators (Van der Pol) with noise, we do not observe dynamics as for the weak-coupling regime in the present model composed of a network of networks. Whenever the coupling becomes significant, these oscillatory models, as well as linear dynamical models based on Gaussian stochastic processes [24], all display prominently the 2-cluster behavior as in the strong coupling regime of our model [Fig. 3(b)]. This comparison shows that self-sustained oscillator models may not be as appropriate for the understanding of the interplay between dynamics and structure in the brain as are models formed by hierarchical networks of *excitable* elements.

The present model focuses on the highest network level and represents each cortical area with a one-level SW subnetwork. While the resulting functional correlations are significant, they are relatively low (maximum 0.1–0.2) in the biologically plausible regime. An increase of correlation strength may be achieved by including further levels of clustered network organization representing hypercolumns, columns, and cellular circuits. This representation would allow localized and strong synchronization in some low-level clusters and would broaden significantly the biologically plausible regimes with stronger correlations, as observed experimentally [10]. A carefully extended model could be used to investigate the relative contributions of network topology and task-related network activations to functional brain connectivity and information processing.

Our model of network of networks using excitable elements can be considered as a promising scheme for the detection of hierarchical communities in a broad range of complex systems. Because of the nature of localized signal propagation, it appears to be more efficient than schemes based on oscillators [6], especially when the community structures are not very clear.

[1] S. H. Strogatz, Nature (London) **410,** 268 (2001); R. Albert and A.-L. Barabási, Rev. Mod. Phys. **74,** 47 (2002); S. Boccaletti *et al.*, Phys. Rep. **424,** 175 (2006).

[2] See, e.g., M. Barahona and L. M. Pecora, Phys. Rev. Lett. **89,** 054101 (2002); T. Nishikawa *et al.*, *ibid.* **91,** 014101 (2003); M. Timme, F. Wolf, and T. Geisel, *ibid.* **92,** 074101 (2004); A. E. Motter, C. S. Zhou, and J. Kurths, Europhys. Lett. **69,** 334 (2005); I. Belykh, E. de Lange, and M. Hasler, Phys. Rev. Lett. **94,** 188101 (2005); C. S. Zhou, A. E. Motter, and J. Kurths, *ibid.* **96,** 034101 (2006); E. Oh *et al.*, Phys. Rev. E **72,** 047101 (2005).

[3] E. Salinas and T. J. Sejnowski, Nat. Neurosci. **2,** 539 (2001); P. Fries, Trends Cogn. Sci. **9,** 474 (2005).

[4] C. Song, S. Havlin, and H. A. Makse, Nature (London) **433,** 392 (2005).

[5] S. Jalan and R. E. Amritkar, Phys. Rev. Lett. **90,** 014101 (2003); C. S. Zhou and J. Kurths, Chaos **16,** 015104 (2006).

[6] A. Arenas, A. Díaz-Guilera, and C. J. Pérez-Vicente, Phys. Rev. Lett. **96,** 114102 (2006).

[7] J. W. Scannell *et al.*, Cereb. Cortex **9,** 277 (1999).

[8] O. Sporns *et al.*, Trends Cogn. Sci. **8,** 418 (2004).

[9] C. J. Stam and E. A. de Bruin, Hum. Brain Mapp. **22,** 97 (2004).

[10] C. J. Stam, Neurosci. Lett. **355,** 25 (2004); V. M. Eguíluz *et al.*, Phys. Rev. Lett. **94,** 018102 (2005); R. Salvador *et al.*, Cereb. Cortex **15,** 1332 (2005).

[11] O. Sporns and J. D. Zwi, Neuroinformatics **2,** 145 (2004).

[12] C. C. Hilgetag and M. Kaiser, Neuroinformatics **2,** 353 (2004).

[13] C. C. Hilgetag *et al.*, Phil. Trans. R. Soc. B **355,** 91 (2000).

[14] M. E. J. Newman and M. Girvan, Phys. Rev. E **69,** 026113 (2004).

[15] D. J. Watts and S. H. Strogatz, Nature (London) **393,** 440 (1998).

[16] G. Buzsáki *et al.*, Trends Neurosci. **27,** 186 (2004).

[17] L. F. Lago-Fernández *et al.*, Phys. Rev. Lett. **84,** 2758 (2000); N. Masuda and K. Aihara, Biol. Cybern. **90,** 302 (2004).

[18] M. P. Young, Spatial Vision **13,** 137 (2000).

[19] R. FitzHugh, Biophys. J. **1,** 445 (1961); A. S. Pikovsky and J. Kurths, Phys. Rev. Lett. **78,** 775 (1997).

[20] R. Kandel, J. H. Schwartz, and T. M. Jessell, *Principles of Neural Science* (McGraw-Hill, New York, 2000).

[21] P. Kudela, P. J. Franaszczuk, and G. K. Bergey, Biol. Cybern. **88,** 276 (2003).

[22] We symmetrize the P1 links in the anatomical matrix M^A for a comparison with the symmetrical functional matrix M^F. The Hamming distance H is the percentage of the nonidentical elements between M^A and M^F.

[23] F. H. Lopes da Silva *et al.*, Kybernetik **15,** 27 (1974).

[24] O. Sporns, G. Tononi, and G. M. Edelman, Cereb. Cortex **10,** 127 (2000).